Composites: Part B 72 (2015) 87–96

Contents lists available at ScienceDirect

Composites: Part B

journal homepage: www.elsevier.com/locate/compositesb

Fatigue crack growth in CFRP-strengthened steel plates

Pierluigi Colombi *, Giulia Fava, Lisa Sonzogni

Department of Architecture, Built Environment and Construction Engineering, ABC Politecnico di Milano, P.zza L. da Vinci, 32, 20133 Milan, Italy

ARTICLE INFO

Article history:
Received 29 July 2014
Received in revised form 7 November 2014
Accepted 28 November 2014
Available online 5 December 2014

Keywords:
A. Carbon fiber
B. Fatigue
B. Debonding
C. Finite element analysis (FEA)

ABSTRACT

In this paper fatigue crack growth in steel plates reinforced by using carbon fiber reinforced (CFRP) strips is investigated from the experimental, numerical and analytical point of view. Single edge notched tension (SENT) specimens were strengthened with different reinforcement configurations and tested at a stress ratio *R* of 0.4. Different initial damage levels were considered and the experimental results showed that the reinforcement application can effectively reduce the crack growth rate and significantly extend the fatigue life. Numerical models (finite elements) were also developed to evaluate the stress intensity factor (SIF) and the crack opening displacement (COD) profile. Based on the numerical results, an analytical model was proposed to predict the fatigue crack growth rate and the fatigue crack growth curves. The analytical results are validated by comparing the fatigue crack growth curves to the experimental ones.

1. Introduction

1.1. Problem statement

Fatigue failure is a very common failure mode for steel structures in the civil engineering field (e.g. road and railway bridges, towers, tanks, pipelines and crane supporting structures). Fatigue loading in stress concentration zones leads to nucleation and growth of cracks. Old steel structures present then fatigue defects that should be repaired in order to extend the relevant service life. Additionally, structures need to be strengthened due to the loading condition increment required by recent standards and guidelines. Due to the above reasons, efficient repair techniques are required to retrofit old steel structures subjected to repeated loading. Traditional techniques such as welding or steel plate bolting are not effective since they are time consuming and costly. Besides, they often introduce new areas of stress concentration and increase the self-weight of the structure.

All the disadvantages of the mentioned traditional repair techniques can be mitigated by the use of composite materials such as the carbon fiber reinforced polymers (CFRP). Such a reinforcing strategy offers the possibility to overcome the existing problems connected to the traditional reinforcing techniques. Despite the higher material cost, due to the unique properties of composite materials (low self-weight, high strength and stiffness and good durability), the strengthening operation can be quickly realized reducing the global rehabilitation costs.

With specific reference to fatigue damaged structures, CFRP reinforcements can reduce crack growth extending then the fatigue life acting in three different ways:

- By reducing the stress range around the crack tip.
- By reducing the crack opening displacement (COD); i.e. CFRP materials bonded to the crack bridge the crack lips and moderate the COD.
- By promoting crack closure; i.e. the reduction of the COD produced by crack patching promotes crack closure.

It is then clear that the patch stiffness plays a very important role in the fatigue reinforcement of steel elements. High stiffness reinforcing materials result, in fact, in a significant decrease of the stress range around the crack tip and in a marked reduction of the COD which promotes crack closure. Crack closure is also emphasized by the eventual pre-stressing of the CFRP strips since the compressive stresses reduce the stress ratio promoting crack closure. Finally, the patch location also plays a role in the fatigue life increment. On the other hand, high patch stiffness produces high interface shear stresses promoting patch debonding or delamination and reducing the reinforcement effectiveness.

The use of CFRP wraps and strips was recently suggested for the reinforcement of steel structures [1–3]. Guidelines are also available [4,5] in order to help in the design of CFRP repaired steel structures. In particular, CFRP reinforcements significantly improve the local structural response through a significant increment of the local stiffness and strength. This is particularly appealing for fatigue reinforcement, as shown by several research programs in the literature from the experimental, analytical and numerical point of view

* Corresponding author. Tel.: +39 0223994280.
E-mail address: pierluigi.colombi@polimi.it (P. Colombi).

http://dx.doi.org/10.1016/j.compositesb.2014.11.036
1359-8368/

[6,7]. Comparative studies were also performed in Jiao et al. [8] to estimate the effectiveness of different retrofitting techniques with composite materials (pultruded CFRP strips and wet layup CFRP sheets) to traditional welding repair. The fatigue life of beams strengthened with CFRP plates or CFRP sheets was significantly longer than that of beams repaired with welding method alone. More recently, FRP materials were also used to repair welded joints [9]. The effect of fatigue life enhancement was evident, indicating that fatigue strength can be upgraded by using composite reinforcements.

1.2. Scope of the research

In this work, crack growth of CFRP-strengthened steel plates is investigated from the experimental, numerical and analytical point of view. Single edge notched tension (SENT) specimens reinforced on a single side by using CFRP strips are considered. In the literature, in fact, center cracked tension (CCT) is often used to investigate the effectiveness of the fatigue strengthening by using composite materials. This small scale specimen configuration is representative of the real situation of a crack emanating from the rivet hole of riveted steel elements, such as road or railway steel bridges. Besides, other reinforcing configurations are worth of investigation such as the crack emanating from the lateral side of the tension flange of a steel beam under cyclic bending loading. This arrangement can be efficiently investigated by using small scale samples realized by SENT specimens. Additionally, the reinforcing material can be often applied, due to several reasons, just to one side of the tension flange. Such a reinforcing configuration is clearly un-symmetric and then the bending effect and the variation of the stress distribution and fracture mechanics parameters through the thickness should be taken into account. Finally, the use of reinforcing strips promotes the crack closure effect by reducing the COD. This has a significant effect on the fatigue crack propagation and fatigue life and it was not up to now in the authors' opinion adequately investigated in the literature. In order to analyze the efficacy of the fatigue repair of the tension flange of a steel beam, small scale experimental tests were performed at the laboratory of the Politecnico di Milano. In particular, SENT specimens were prepared and reinforced by using a single CFRP reinforcing configuration. The achieved fatigue crack growth curves allowed investigating the reinforcement arrangement efficacy on the crack propagation rate and then the fatigue lifetime.

1.3. Previous studies

Fundamental researches were focused on the effectiveness of the fatigue reinforcement of steel plates strengthened by using CFRP wraps and strips. Jones and Civjan [10] analyzed the fatigue behavior of steel plates notched either from a central hole or from the edges (double edge notched tension) with respect to the CFRP system and bond geometry. The effects of one or two side reinforcements and of an application prior or subsequent to crack propagation were also taken into account. Colombi et al. [11] showed that the application of pre-stress bonded composite patches is a promising technique to reinforce notched steel plates damaged by fatigue. The application of CFRP strips and, eventually, the pretension of the strips prior to bonding remarkably increased the remaining fatigue life. Liu et al. [12,13] investigated the effects of patch system, thickness, length, width, and patch configurations on single- and double-sided repaired steel plates.

The prediction of the fatigue life of CFRP-strengthened steel plates was studied by Liu et al. [13]. An analytical model was developed to predict the fatigue behavior of steel plates repaired by using composite materials. The analytical model was verified by experimental results. In Wang and Nussbaumer [14], the concept of fracture mechanics was extended to the fatigue crack propagation of cracked steel plates reinforced by using a composite patch. A formula connecting the stress intensity factor (SIF) to the crack length of the repaired steel plate was first derived. Thereafter, a fracture model for the fatigue crack propagation was proposed and verified by test data. The effect of the CFRP strips on the fatigue crack growth rate was also investigated in Colombi [15]. In particular, a model capable to predict the effect of crack closure on the fatigue life was developed. The effect of the CFRP strip pre-tension level on the repair efficacy was also investigated. Tsouvalis et al. [16] considered CCT specimens reinforced by a CFRP patch on a single side. Results showed that the reinforcement patches, despite their relatively low stiffness ratio, can effectively extend the fatigue life by a factor of two. In several studies, the fatigue behavior of notched steel members reinforced by using prestressed CFRP laminates is considered. Prestressed reinforcements were observed to be more effective in extending the crack growth life [11,17,18]. Crack patching by prestressed CFRP strips produces, in fact, supplementary benefits since the compressive stresses introduced by prestressing the steel elements give rise to an additional reduction of the COD and emphasize the crack closure phenomenon. More recently, fatigue tests by Wu et al. [19] revealed that ultra-high modulus (UHM) CFRP plates are very effective for the fatigue strengthening of cracked steel plates. Yu et al. [20] considered three different artificial crack lengths to simulate the effect of increasing fatigue damage levels on notched steel plates with a hole and two initial cracks in the center. The experimental results showed that the CFRP patches could effectively slow down the crack growth and extend the fatigue life. In Yu et al. [21] much wider damage levels were considered. Different reinforcing materials (normal modulus and ultra-high modulus CFRP reinforcement) were also considered together with two types of reinforcing schemes. The output was that it is recommended to adopt an early repair of the cracked steel plate. The effect of initial damage and reinforcement configurations was also investigated by Wang et al. [22]. Results showed that the repair efficacy was highly dependent from CFRP thickness, initial crack length, reinforcement arrangement and local debonding size.

A peculiar aspect of the CFRP reinforcement of steel structures is that the adhesive layer is the weakest point of the system due to the very high strength of the steel substrate. Reinforcement debonding is then the dominant failure mode of strengthened steel member. In particular for fatigue strengthening crack mouth, debonding plays an important role as clearly demonstrated in [23–25]. The presence of a debonded area in the crack tip region significantly reduces the effectiveness of the reinforcement technique and should be taken into account in the evaluation of the fatigue lifetime.

2. Experimental tests

The experimental program was conducted at the Materials Testing Laboratory of the Politecnico di Milano. A total of 10 specimens were prepared and tested. One unreinforced specimen was used as control specimen, while 9 additional specimens were tested to investigate the effects of reinforcement stiffness, reinforcement configuration and initial damage level. Specimens were 450 mm long, 50 mm wide and 8 mm thick. The geometry and dimensions of the SENT specimens are illustrated in Fig. 1. The specimens were machined with a side notch consisting of a slot 5 mm long and 0.20 mm wide (see Fig. 1). The slots were prepared by electric discharging machining (EDM).

2.1. Specimen configurations

Different parameters, as the initial crack length when the steel plate is reinforced and the patch configuration (reinforcement

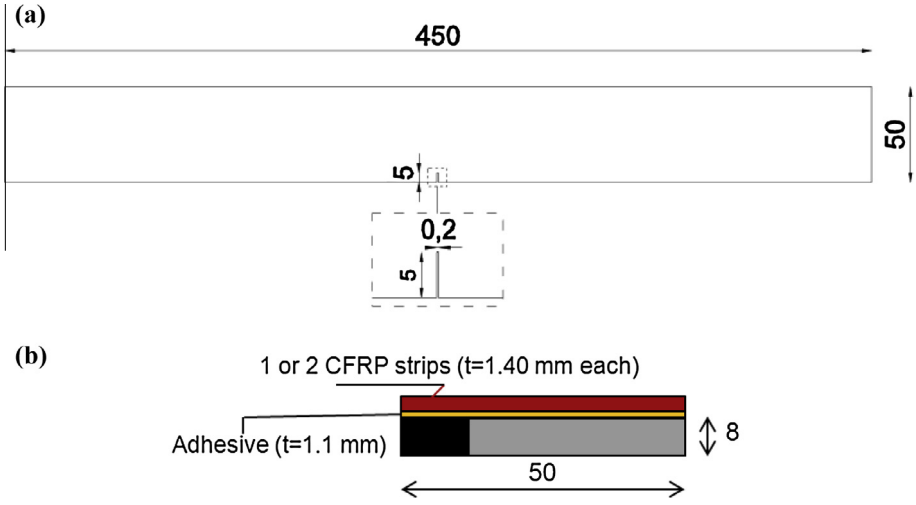

Fig. 1. SENT specimen geometry: (a) steel plate and (b) specimen reinforcement.

amount and location), were investigated. For simulating different degrees of damage, two values were considered for the initial crack length when the steel plate is reinforced, i.e. 6 mm and 15 mm. The initial damage level is then characterized by the value of α, the ratio between the initial crack length and the plate width W (W = 50 mm). The selected initial crack lengths correspond to an initial damage level of 12% and 30%, respectively.

Concerning the patch configuration, two reinforcement amounts are considered, i.e. a thickness of 1.4 mm corresponding to the application of one CFRP layer and a patch thickness of 2.8 mm for specimens reinforced with two CFRP layers.

Different patch locations were finally considered as the fully or partially covered steel plates, as shown in Fig. 2. Case (a) represents the steel plate fully covered by the patch and it is considered as the reference reinforcing configuration. Case (b) is the steel plate partially bonded by the patch on the lateral side. In this case the crack is covered by the patch for a crack length up to 25 mm, i.e. half of the steel plate width.

Details of the experimental program are presented in Table 1 where a_i is the initial crack size of the reinforced specimen and t_p is the patch thickness, α is the initial damage level and R_G is the reinforcement ratio, defined as the ratio between the patch and the steel plate section:

$$R_G = \frac{E_p \cdot A_p}{E_s \cdot A_s} \tag{1}$$

In Eq. (1), E_s is the steel Young's modulus, E_p is the patch Young's modulus along the longitudinal (specimen) axis, while A_p and A_s are the patch and steel sections, respectively. The ratio R_G characterizes the amount of reinforcement applied to the steel plates and the axial stiffness of the reinforced steel plates.

Uniaxial sinusoidal loading cycles were applied at a loading frequency of 18 Hz. All the specimens were tested under constant amplitude tensile loading with a maximum and minimum load of 60 kN and 24 kN, respectively. The corresponding loading ratio R is equal to 0.4.

2.2. Materials and specimen preparation

Specimens were prepared using steel plates of type S275J0, according to the European standards. Steel mechanical properties were determined through tensile coupon tests. The mean yielding stress and tensile strength were of 330 MPa and 444 MPa, respectively. The Young's modulus was of 208 GPa. The reinforcements were CFRP strips (Sika CarboDur® M514) with a thickness of 1.4 mm. The nominal values of the Young's modulus and tensile strength were greater than 200 GPa and 2800 MPa, respectively. The Young's modulus was assumed equal to 210 GPa. The CFRP strips were bonded to the steel plates using a thixotropic epoxy resin (Sikadur® 30) with Young's modulus and tensile strength greater than 4500 MPa and 28.4 MPa, respectively.

For specimens reinforced with two layers of pultruded CFRP strips a less viscous epoxy adhesive (Sikadur® 330) was used to bond the outer CFRP strip to the inner one. The nominal values of the Young's modulus and tensile strength were greater than 3800 MPa and 30 MPa, respectively. The mechanical properties are summarized in Table 2.

Specimens were initially subjected to fatigue loading in order to produce an initial pre-crack of approximately 6 mm. Some specimens were immediately reinforced while other ones were strengthened after being additionally subjected to fatigue loading up to a crack length of approximately 15 mm. The steel plate

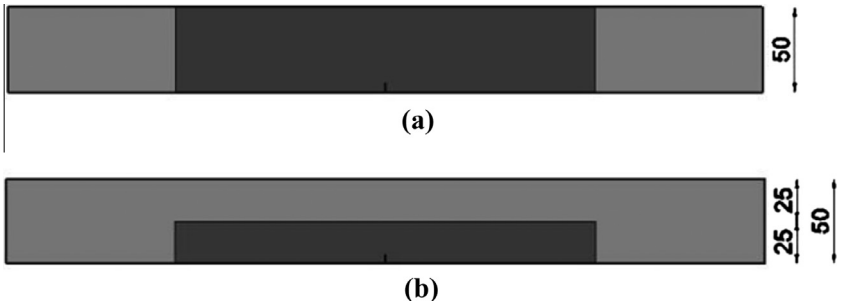

Fig. 2. Patch configurations of type (a) and (b).

Table 1
Detail of the experimental program and fatigue results.

Specimens	Patch conf.	a_i (mm)	t_p (mm)	α (%)	R_G (/)	N_i^{steel}	N_f^{steel}	N_f^{CFRP}	R_N (/)
U-D12	/	6	/	12	/	0	196,714	/	/
		15	/	30	/	0	29,264	/	
A2-D12-1	a	6.1	2.8	12	0.353	0	196,714	584,000	2.97
A2-D12-2	a	6.4	2.8	12	0.353	0	196,714	565,000	2.87
A2-D12-3	a	6	2.8	12	0.353	0	196,714	605,000	3.08
A2-D30-1	a	14.8	2.8	12	0.353	173,416	29,264	172,000	1.70
A2-D30-2	a	14.9	2.8	30	0.353	179,000	29,264	133,000	1.50
A1-D12	a	6	1.4	30	0.176	0	196,714	512,500	2.61
A1-D30	a	14.7	1.4	30	0.176	187,000	19,216	77,000	1.22
B1-D30	b	14.8	1.4	30	0.088	179,000	29,216	66,800	1.18
B2-D30	b	15.0	2.8	30	0.176	186,000	29,216	100,000	1.32

Patch conf. = patch configuration type (see Fig. 2).
a_i = initial crack size.
t_p = reinforcement thickness.
α = initial damage level.
R_G = reinforcement ratio.
N_i^{steel} = number of cycles to the initial crack size (steel only).
N_f^{steel} = number of cycles to failure (steel only).
N_i^{CFRP} = number of cycles to failure (CFRP reinforced specimen).
R_N = fatigue life increase ratio.

surfaces were firstly treated to remove the rust and to create a rough surface. Then the CFRP strips were cut to a proper length and bonded after preparing the steel surface. The two components of the epoxy adhesive (Sikadur® 30) were dosed, mixed and distributed on the CFRP surface. Then, the CFRP strips were pressed on the steel substrate and the adhesive in excess was removed. For specimens reinforced with two CFRP layers, the adhesive (Sikadur® 330) was distributed on the composite material and the CFRP strips were pressed. Finally, the specimens were cleaned and subjected to uniform pressure by applying dead weights on the CFRP surface. After two days the dead weights were removed and the bond line was visually inspected. The adhesive thickness was approximately of 1.1 mm.

3. Fatigue results

Observed failure was mainly due to debonding at the steel/adhesive interface and sudden static failure of the steel plate. The crack size in the steel plate at debonding was of about 35–40 mm (70–80% of the specimen width). The experimental results are presented in Table 1 in terms of the number of cycles to failure and the fatigue life increment ratio, R_N, defined as:

$$R_N = \frac{N_i^{steel} + N_f^{CFRP}}{N_i^{steel} + N_f^{steel}} \quad (2)$$

where N_i^{steel} is the number of cycles to the initial crack size prior to bonding for the reinforced specimen, N_f^{steel} is the number of cycles to failure for the unreinforced specimen (specimen P06) and N_f^{CFRP} is the number of cycles to failure for the reinforced specimen. In Eq. (2) it is explicitly taken into account the number of cycles required for the initial crack formation in order to highlight the effect of the initial damage on the fatigue performance [21]. For long initial crack size, in fact, the initial crack formation accounts for a considerable portion of the whole fatigue life.

Table 2
Materials parameters from experimental tests.

	Young's modulus	Yield stress	Tensile strength
Steel	208 GPa	330 MPa	444 MPa
CFRP	>200 GPa		>2800 MPa
Adhesive	>4500		>28.4 MPa

The analysis of Table 1 indicates that:

- For short initial cracks, Case (a) reinforcement type and two reinforcement layers (specimen type A2-D12), a mean fatigue life increase ratio equal to 2.97 was achieved. Single layer reinforcement (specimen A1-D12) is moderately less efficient since a fatigue life increase ratio was equal to 2.61.
- For long initial cracks, Case (a) reinforcement type and two reinforcement layers (specimen type A2-D30), a mean fatigue life increase ratio equal to 1.60 was achieved. A single layer reinforcement configuration (specimens A1-D30) is less efficient with a fatigue life increase ratio equal to 1.22.
- For long initial cracks, Case (b) reinforcement type and two reinforcement layers (specimen B2-D30) a fatigue life increase ratio equal to 1.32 was attained. A single layer reinforcement configuration (specimen B1-D30) is moderately less efficient with a fatigue life increase ratio equal to 1.18.

As a preliminary conclusion, the repair of long initial crack size is much less efficient then the case of short initial crack size. Early repair is then suggested in order to achieve the best fatigue life increment of the damaged steel plate. This means that the repair is much more efficient for specimens with short initial crack size. Two layers arrangement and Case (a) reinforcement configuration are the most efficient reinforcement arrangement. Besides, Case (b) reinforcement configuration provides a quite good fatigue performance if a sufficient amount of reinforcement stiffness is adopted. This means that if thicker reinforcement is applied and the patch fully covers the crack, a significant fatigue life enhancement is attained.

3.1. Crack propagation curves

The fatigue crack propagation curve is reported in Fig. 3 where the crack length is plotted against the number of cycles for the tested specimens.

The results in Fig. 3 clearly demonstrate that the fatigue life increment ratio strongly depends from the initial crack size. In fact, the fatigue strength is higher for short initial crack size compared to long initial crack size. The best fatigue performance was observed for specimen type A2 for both the investigated initial damage levels. In particular, a significant fatigue life increment ratio is achieved for short initial crack size (specimens type A2-D12) while a moderate increment of the fatigue performance is

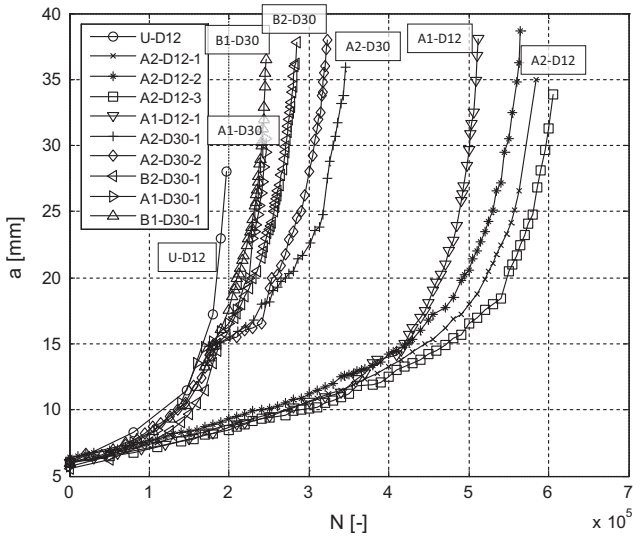

Fig. 3. Crack propagation curves.

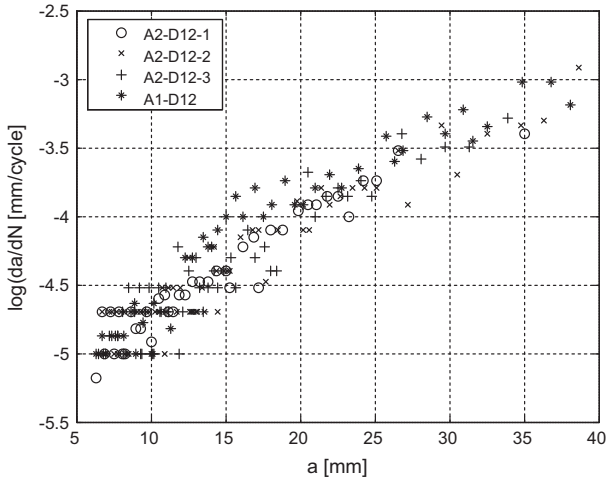

Fig. 4. Crack growth rate for short initial crack size (specimen type A2-D12 and A1-D12).

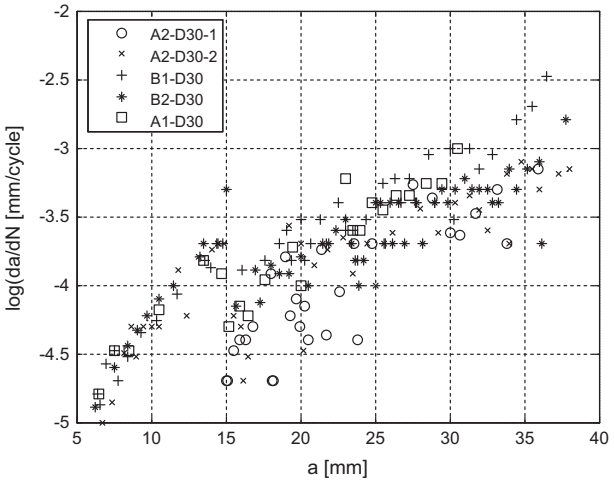

Fig. 5. Crack growth rate for long initial crack size (specimen type A2-D30, A1-D30, B1-D30 and B2-D30).

attained for long initial crack size and one layer reinforcement configuration (specimens type A1-D30 and B1-D30).

3.2. Crack propagation rates

The experimental fatigue crack growth rate is evaluated by using the "secant method" suggested in ASTM E 647 [26]:

$$\left(\frac{da}{dN}\right)_{\bar{a}} = \frac{(a_{i+1} - a_i)}{(N_{i+1} - N_i)} \tag{3}$$

Eq. (3) represents an average crack growth rate in the interval $[a_i - a_{i+1}]$, corresponding to the average crack length $\bar{a} = \frac{1}{2}(a_{i+1} - a_i)$. Crack propagation rates for specimens with short initial crack size are reported in Fig. 4.

This figure clearly indicates that two reinforcement layers and configuration (a) (specimen type A2-D12) are the most efficient strengthening arrangement. A lower crack growth rate decrement is in fact obtained with one layer reinforcement (specimen A1-D12).

Crack propagation rate for specimens with long initial crack size are reported in Fig. 5.

In the first part of the fatigue crack propagation, the specimens were unreinforced and the CFRP patch was applied at a crack size of 15 mm. The effect of the reinforcement is evident from Fig. 5 and it results in a significant decrement of the fatigue crack growth rate. This is more evident for specimen type A2-D30, i.e. for configuration (a) and two reinforcement layers and it less pronounced for specimens A1-D30, i.e. configuration (a) and one reinforcement layer. Configuration (b) and two reinforcement layers is clearly less efficient (specimen B2-D30) than configuration (a) and this is more evident in the case of one reinforcement layer (specimen B1-D30).

4. Numerical modeling

A numerical model was used to simulate the experimental tests. A two-dimensional finite element model was developed for reducing the computational effort. The commercial finite element code ABAQUS was used. The geometric model contains three parts: the steel plate, the adhesive layer and the CFRP reinforcement. To detect the strain singularity at the crack tip, a special mesh with proper elements was used, allowing to the calculation of the SIF in the steel. Four-node shell elements (S4R) and the mesh were assembled as follows: 18,595 nodes and 18,176 elements for the steel plate; 6,526 nodes and 6,250 elements for both the adhesive and the composite reinforcement. Quarter point elements were used at the crack tip to pick up the strain singularity and allow the calculation of the SIF for the steel. The number of singular elements in the circumferential direction at the crack tip was equal to 10, resulting from a corresponding parametric study.

The finite-element analyzes are performed by applying on the steel plate edges an increasing tensile stress corresponding to the maximum fatigue loading. The constitutive laws are set to be linear elastic. The steel plate has Young's modulus and Poisson ratio equal to 208 GPa and 0.3 respectively. The CFRP reinforcement has Young's modulus and Poisson ratio of 210 GPa and 0.3 respectively. The adhesive has Young's modulus and Poisson ratio of 4.5 GPa and 0.3 respectively.

Debonding is assumed to occur at the adhesive–steel interface [27]. Based on the experimental evidence, a semi-elliptical shape as in Fig. 6(a) was assumed for the debonded area. The major semi-axis was set equal to the crack size, a, while the minor semi-axis lies at the specimen edge, perpendicular to the crack. It was finally supposed that the aspect ratio of the debonded area is equal to 1/5. In the numerical model the debonded area was modeled, for sake of simplicity, as in Fig. 6(b).

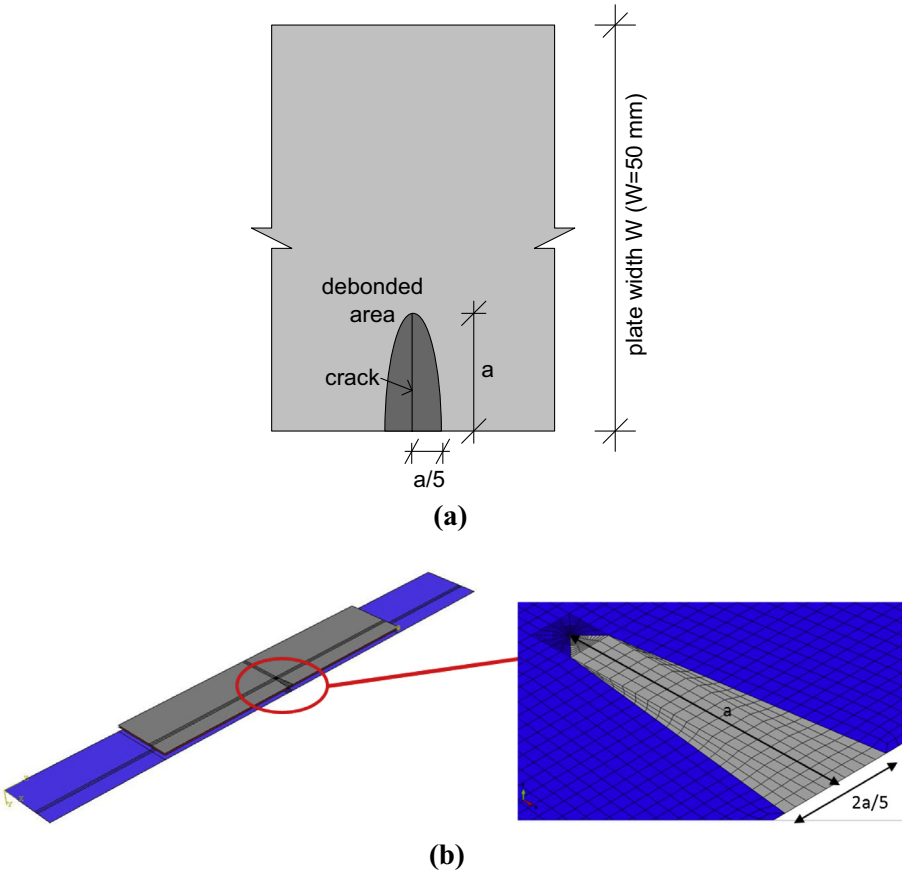

Fig. 6. (a) Debonded area (not to scale) close to the crack region and (b) finite element model and mesh detail in the debonded area.

4.1. SIF evaluation and COD assessment

SIF values were extracted from the FE models for different crack lengths. The numerical results are reported in Fig. 7 with reference to Case (a) reinforcement configuration. Analytical solution refers to [28].

The SIF values for the reinforced steel plates are significantly lower than the ones for the unreinforced specimen and no significant difference is noticed between one layer and two layers reinforcement configuration.

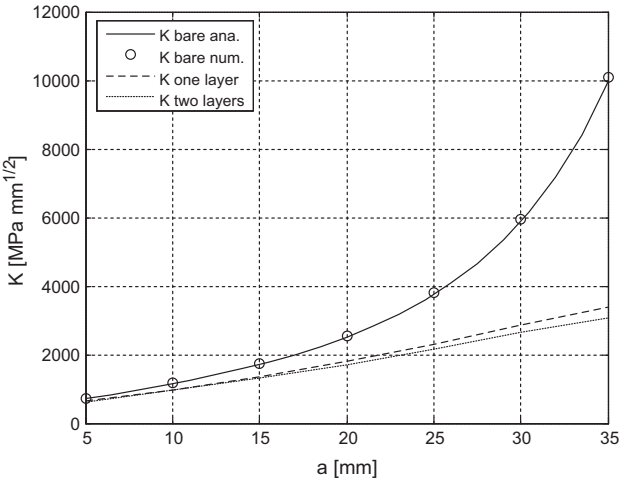

Fig. 7. Maximum stress intensity factor (P = 60 kN) for the bare and reinforced steel plate (one layer and two layers) and Case (a) reinforcement configuration.

The COD was also evaluated from the numerical model and Fig. 8 shows the COD with reference to a 20 mm long initial crack size and Case (a) reinforcement configuration.

The COD values for the reinforced steel plates are significantly lower than the ones for the unreinforced steel plate and no significant difference is observed between one layer and two layers reinforcement configuration. The results in Figs. 7 and 8 clearly illustrate that a similar behavior for one layer and two layer reinforcement configuration is expected in term of fatigue life increment ratio. This is confirmed by considering the fatigue crack propagation curves in Fig. 3 and the numerical values of Table 1.

5. Crack growth life prediction

5.1. Fatigue crack growth law

Linear elastic fracture mechanics concepts are used to investigate the fatigue crack growth. In particular, Paris law is widely used to predict the crack growth rate. In this paper the following modified version of the Paris law is adopted [12]:

$$\frac{da}{dN} = C \cdot \left(\Delta K_{eff}^{m} - \Delta K_{eff,th}^{m}\right) \tag{4}$$

where a is the crack size, N is the number of duty cycles, ΔK_{eff} is the effective SIF range, $\Delta K_{eff,th}$ is the effective threshold SIF range and C and m are material parameters (Paris constants). The crack growth rate is assumed to be equal to zero (no crack growth) for a stress range lower than the threshold stress range. In other words, there is no crack propagation for a stress range lower than the threshold stress range. During the fatigue life the crack experiences crack closure. This means that premature contact of the crack face is

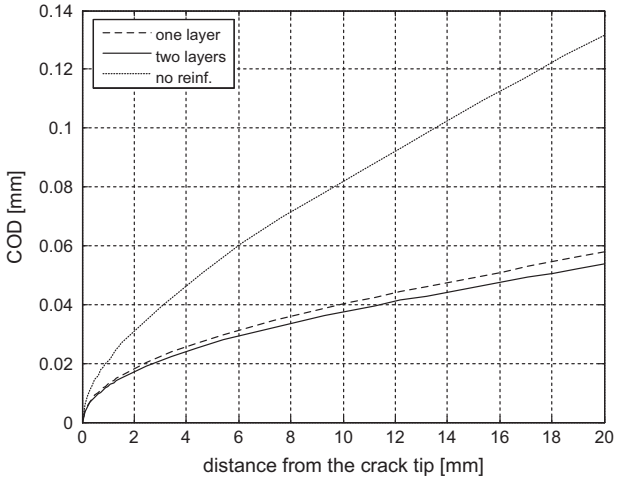

Fig. 8. Crack opening displacement (COD) for the bare and reinforced steel plate (one layer and two layers) and Case (a) reinforcement configuration.

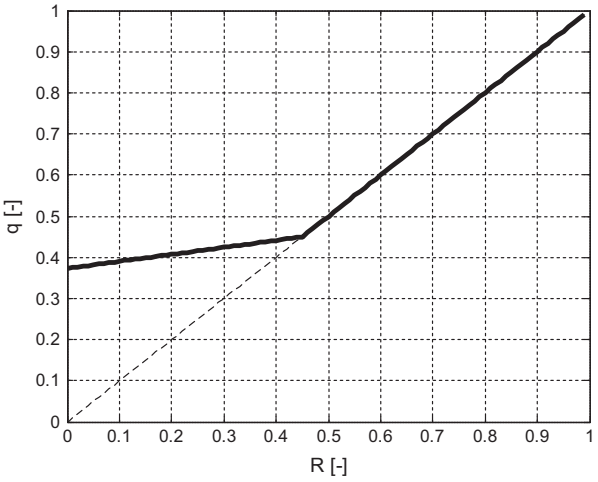

Fig. 9. Relationship between the effective stress ratio (q) and the applied stress ratio (R).

achieved during the unloading branch of the duty cycle. It is then postulated that the crack does not act as stress concentrator if the stress is lower than the so called opening stress. Only when the opening stress is reached, the crack becomes fully opened and the fatigue crack propagation is then possible. This means that just a portion of the stress range, the so called effective stress range, is then effective for crack propagation. The effective SIF range, ΔK_{eff}, is the defined as:

$$\Delta K_{eff} = K_{max} - K_{op} = (1 - q) \cdot K_{max} \tag{5}$$

where q is the effective stress ratio:

$$q = \frac{\sigma_{op}}{\sigma_{max}} \tag{6}$$

and K_{op} is the opening SIF, i.e. the SIF level at which the crack become fully opened. The effective stress ratio is computed by the following expression [28]:

$$q = max\left[\frac{1}{1 + pcf}(1 + R \cdot R_{ys}), R\right] \tag{7}$$

where $R = \sigma_{min}/\sigma_{max}$ is the stress ratio, $R_{ys} = \sigma_{max}/\sigma_y$ is the yield stress ratio (σ_y is the yield stress) and pcf is the plastic constraint factor. The plastic constraint factor takes into consideration the thickness effect on fatigue crack growth. In Fig. 9, the effective stress ratio, q, is plotted as a function of the stress ratio, R, for $pcf = 1.68$ and $\sigma_y = 330$ MPa.

5.2. Estimation of the fatigue crack growth parameters

Experimental data on the bare steel plate are used to calibrate the parameters of the fatigue crack propagation law (see Eq. (4)). At first, the fatigue crack growth rate is determined using the relationship given in Eq. (3). Then, after some algebra, the experimental effective SIF range can be evaluated from Eq. (4) as:

$$\frac{1}{m}\left\{\log\left[\left(\frac{da}{dN}\right)_{\bar{a}} + C\Delta K_{eff,th}^{m}\right] - \log(C)\right\} = \log(\Delta K_{eff}) \tag{8}$$

The effective SIF range, ΔK_{eff}, is estimated by using Eq. (5) and the finite element results for the SIF range, ΔK (see also Fig. 7). The effective stress ratio, q, is calculated by using Eq. (7) and the materials parameters listed in Table 2. The non-linear least square method and the software MATLAB are finally used to evaluate the best fit of parameters C, m and $\Delta K_{eff,th}$ in Eq. (8) by adopting as independent variable the average crack growth rate and as dependent variable the effective SIF range. The results in term of the unknown parameters are reported in Table 3.

Table 3
Estimated fatigue crack growth parameters.

ΔK_{th} (MPa $\sqrt{}$mm)	C	m
161.8	2.669e−014	3.307

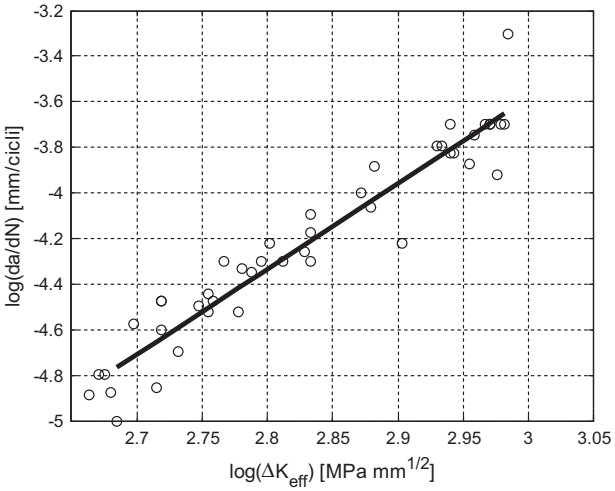

Fig. 10. Relationship between the crack growth rate and the effective stress intensity factor range for the bare steel plate.

The calibrated fatigue crack propagation law (see Eq. (4) and Table 3) is compared to experimental data in Fig. 10.

6. Numerical results

6.1. Fatigue crack growth rate

As clearly illustrated in Fig. 8, the COD for the reinforced steel plates is significantly lower than the unreinforced one. It is then expected that the crack closure effects are more pronounced for reinforced specimens than for the unreinforced ones. Premature contact of the crack faces is, in fact, more likely for reinforced

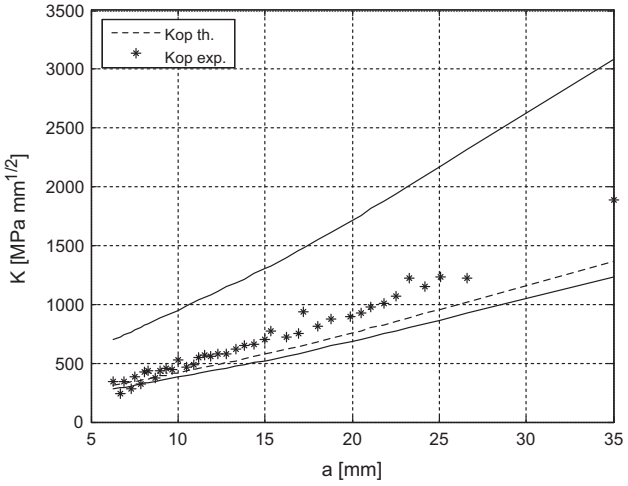

Fig. 11. Opening stress intensity factor for specimen A2-D12-1.

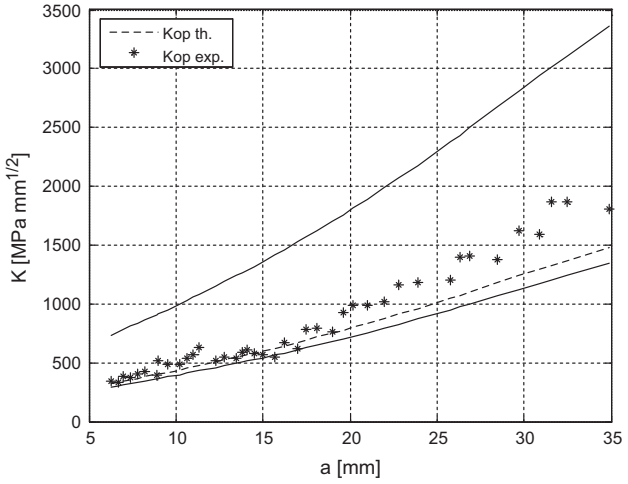

Fig. 12. Opening stress intensity factor for specimen A1-D12.

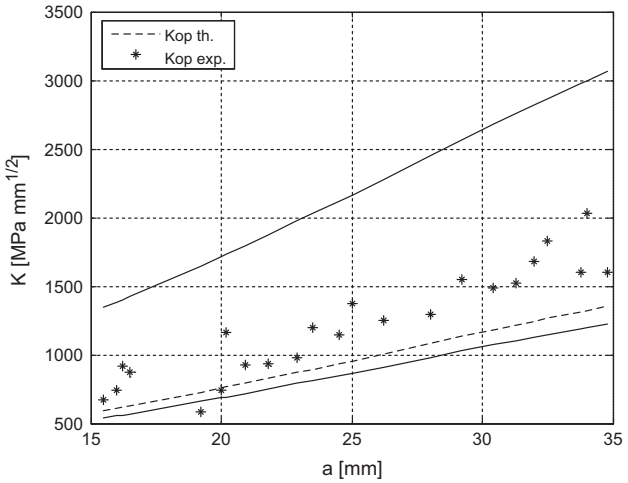

Fig. 13. Opening stress intensity factor for specimen A2-D30-2.

specimens and may result in a high opening SIF, K_{op}. In order to investigate the effect of the reinforcement on the effective stress ratio, the experimental opening SIF is evaluated from Eq. (5) as:

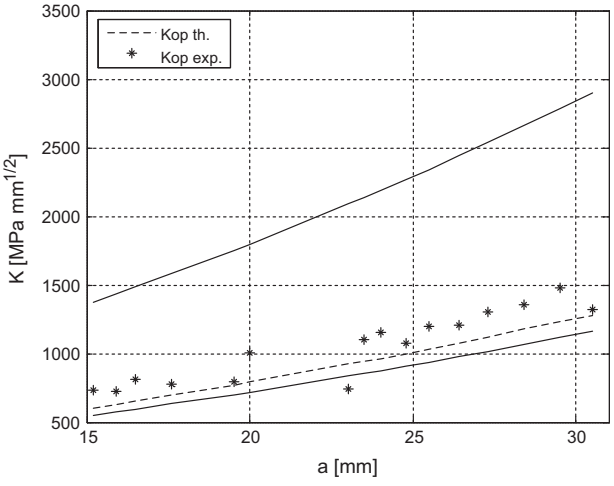

Fig. 14. Opening stress intensity factor for specimen A1-D30.

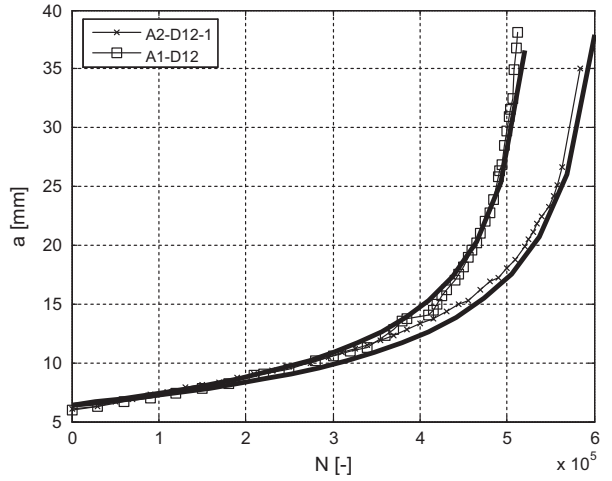

Fig. 15. Predicted and experimental crack growth curves for specimens A2-D12-1 and A1-D12.

$$K_{op} = K_{max} - \Delta K_{eff} \tag{9}$$

where K_{max} is computed from the finite element results (see also Fig. 7) and the experimental ΔK_{eff} is evaluated from Eq. (8). Results are plotted in Figs. 11–14 as function of the crack length.

In the above figures, the upper and lower solid curves represent the SIF at the maximum and minimum load level, respectively.

These figures clearly show that Eq. (7) underestimate the opening SIF range, especially for long cracks. Assuming, for sake of simplicity, a constant effective stress ratio, q, independent from the crack size, the following corrected expression is then proposed:

$$q = \beta \cdot max\left[\frac{1}{1+pcf}(1 + R \cdot R_{ys}), R\right] \tag{10}$$

where β is an experimental corrector factor to be estimated from the experimental results.

6.2. Fatigue life

The predicted fatigue life N_f is evaluated by the numerical integration of Eq. (4) as:

$$N_f = \int_{a_i}^{a_f} \frac{da}{C \cdot (\Delta K_{eff}^m - \Delta K_{eff,th}^m)} \tag{11}$$

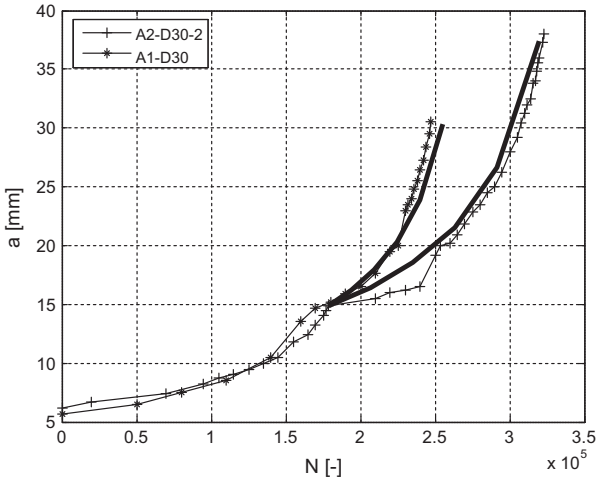

Fig. 16. Predicted and experimental crack growth curves for specimens A2-D30-2 and A1-D30.

where C, m and $\Delta K_{eff,th}$ are the Paris constants listed in Table 3 and ΔK_{eff} is the effective SIF range (see Eq. (5)). The Paris law is integrated between the initial crack size a_i and the final crack size a_f. The effective SIF range is evaluated by using Eqs. (5) and (10). In particular, the effective stress ratio q is evaluated by means of Eq. (10) with an experimental corrector factor $\beta = 1.10$. Results of the numerical integration of the fatigue crack growth law are reported in Fig. 15 for long initial crack size and in Fig. 16 for short initial crack size. The agreement between numerical results and experimental data is satisfactory.

7. Conclusions

The experimental, analytical and numerical study presented in the paper regarded the fatigue behavior of SENT specimens reinforced on a single side by using CFRP strips. On the basis of the experimental campaign and on the corresponding numerical modeling, the present work resulted in interesting conclusions concerning the fatigue behavior of the specimens.

Starting from the experimental results, failure was mainly due to debonding at the steel/adhesive interface and sudden static failure of the steel plate. The crack size in the steel plate at debonding was of about 70–80% of the specimen width. Significant fatigue life increments were observed and the crack repair is noticeably more efficient for short initial crack size, i.e. for small initial degrees of damage. The most efficient reinforcement configuration (specimen type A2-D12) consisted of the steel plate fully covered by the reinforcement (patch configuration (a)). Concerning the influence of the reinforcement ratio on the fatigue repair efficiency (specimen B2-D30), it is interesting to notice a significant increment of the fatigue life increase ratio for long initial crack size and patch configuration (b). Finally there was an effect of the patch position on the fatigue repair efficacy. In fact, patch configuration (b) with an adequate reinforcement ratio (specimen B2-D30) was efficient in the repair of fatigue damaged steel elements.

The numerical model developed in the paper was useful for the interpretation of the experimental results. Debonding phenomena were assumed to occur at the adhesive-plate interface and were modeled by considering an elliptical debonded area. Based on the FE model, the SIF and COD were evaluated for increasing values of the crack length. Both the SIF and the COD for the reinforced steel plates were significantly lower than the unreinforced one, while no significant difference between the reinforcement configurations with one CFRP layer and two layers was noticed. It is then expected that the crack closure effects are more pronounced for reinforced specimens than for the unreinforced ones.

Based on linear elastic fracture mechanics and applying a modified version of the Paris law, theoretical studies of the crack growth in SENT specimens reinforced on a single side by using CFRP strips were performed to predict the fatigue crack growth rate and the fatigue crack growth curves. The parameters of the fatigue crack propagation law were calibrated on the basis of the experimental data for the bare steel plate. A corrected expression for the effective stress ratio, q, is required to allow for the effect of the reinforcement application on the crack closure. For both long initial crack size and short initial crack size, the agreement between analytical results and experimental data was satisfactory.

The analytical model is then considered to be useful and convenient for the estimation of the SIF, crack growth rate and fatigue life of SENT specimens reinforced on a single side by using CFRP strips.

Acknowledgements

The financial support of the Politecnico di Milano is gratefully acknowledged. Thanks are also expressed to Sika Italia spa for providing the pultruded strips and the epoxy adhesive used in the experimental program.

References

[1] Hollaway LC, Cadei J. Progress in the technique of upgrading metallic structures with advanced polymer composites. Progr Struct Mater Eng 2002;4(2):131–48.
[2] Zhao XL, Zhang L. State of the art review on FRP strengthened steel structures. Eng Struct 2007;29(8):1808–23.
[3] Teng JG, Yu T, Fernando D. Strengthening of steel structures with fiber-reinforced polymer composites. J Constr Steel Res 2012;78:131–43.
[4] Cadei JMC, Stratford TJ, Hollaway LC, Duckett WH. C595 – Strengthening metallic structures using externally bonded fibre-reinforced composites. London: CIRIA; 2004.
[5] Schnerch D, Dawood M, Rizkalla S, Sumner E. Proposed design guidelines for strengthening of steel bridges with FRP materials. Constr Build Mater 2007;21(5):1001–10.
[6] Zhao XL. FRP strengthening of metallic structures subject to fatigue loading. In: Proceedings of seventh national conference on FRP in construction, October, Hangzhou, China; 2011. p. 15–6.
[7] Colombi P, Fava G. Fatigue life of steel components strengthened with fibre-reinforced polymer (FRP) composites. In: Karbhari VM, editor. Rehabilitation of metallic civil infrastructure using fiber reinforced polymer (FRP) composites. Cambridge: Woodhead; 2014. p. 239–68 [ISBN: 978-0-85709-653-1].
[8] Jiao HA, Mashiri F, Zhao XL. A comparative study on fatigue behaviour of steel beams retrofitted with welding, pultruded CFRP plates and wet layup CFRP sheets. Thin-Walled Struct 2012;59:144–52.
[9] Chen T, Zhao XL, Gu XL, Xiao ZG. Numerical analysis on fatigue crack growth life of non-load-carrying cruciform welded joints repaired with FRP materials. Compos B 2014;2014(56):171–7.
[10] Jones SC, Civjan SA. Application of fibre reinforced polymer overlays to extend steel fatigue life. J Compos Constr 2003;7(4):331–8.
[11] Colombi P, Bassetti A, Nussbaumer A. Analysis of cracked steel members reinforced by pre-stress composite patch. Fatigue Fract Eng Mater Struct 2003;26(1):59–66.
[12] Liu HB, Al-Mahaidi R, Zhao XL. Experimental study of fatigue crack growth behaviour in adhesively reinforced steel structures. Compos Struct 2009;90(1):12–20.
[13] Liu HB, Xiao ZG, Zhao XL, Al-Mahaidi R. Prediction of fatigue life for CFRP strengthened steel plates. Thin-Walled Struct 2009;47(10):1069–77.
[14] Wang R, Nussbaumer A. Modelling fatigue crack propagation of a cracked metallic member reinforced by composite patch. Eng Fract Mech 2009;76:1277–87.
[15] Colombi P. Plasticity induced fatigue crack growth retardation model for steel elements reinforced by composite patch. Theoret Appl Fract Mech 2005;43(1):63–76.
[16] Tsouvalis NG, Mirisiotis LS, Dimou DN. Experimental and numerical study of fatigue behaviour of composite patch reinforced cracked steel plate. Int J Fatigue 2009;31:1613–27.
[17] Taljsten B, Hansen CS, Schmidt JW. Strengthening of old metallic structures in fatigue with prestressed and non-prestressed CFRP laminates. Constr Build Mater 2009;23(4):1665–77.

[18] Huawen Y, Konig C, Ummenhofer T, Shizhong Q, Plum R. Fatigue performance of tension steel plates strengthened with pre-stressed CFRP laminates. J Compos Constr 2010;14(5):609–15.
[19] Wu C, Zhao XL, Al-Mahaidi R, Emdad M, Duan WH. Fatigue tests of cracked steel plates strengthened with UHM CFRP plates. Adv Struct Eng – Int J 2012;15(10):1801–16.
[20] Yu QQ, Chen T, Gu XL, Zhao XL, Xiao ZG. Fatigue behaviour of CFRP strengthened steel plates with different degree of damage. Thin-Walled Struct 2013;69:10–7.
[21] Yu QQ, Zhao XL, Al-Mahaidi R, Xiao ZG, Chen T, Gu XL. Tests on cracked steel plates with different damage levels strengthened by CFRP laminates. Int J Struct Stab Dyn 2014;14(6):1450018. http://dx.doi.org/10.1142/S0219455414500187.
[22] Wang H, Wu G, Wu Z. Effect of FRP configurations on the fatigue repair effectiveness of cracked steel plate. J Compos Constr 2014. http://dx.doi.org/10.1061/(ASCE)CC.1943-5614.0000422.
[23] Colombi P, Bassetti A, Nussbaumer A. Delamination effects on cracked steel members reinforced by prestressed composite patch. Theoret Appl Fract Mech 2003;39:61–71.
[24] Aggelopoulos ES, Righiniotis TD, Chryssanthopoulos MK. Debonding of adhesively bonded composite patch repairs of cracked steel members. Compos B Eng 2011;42(5):1262–70.
[25] Wu C, Zhao XL, Chiu WK, Al-Mahaidi R, Duan WH. Effect of fatigue loading on the bond behaviour between UHM CFRP plates and steel plates. Compos B Eng 2013;2013(50):344–53.
[26] ASTM E647. Standard test method for measurement of fatigue crack growth rates. Annual book of ASTM standards. West Conshohocken: ASTM; 2001.
[27] Bassetti A. Lamelles pre-contraintes en fibres de carbone pour le renforcement de ponts rivètes endommages par fatigue (in French). PhD thesis. Swiss Federal Institute of Technology, EPFL, Switzerland; 2011.
[28] Tada H, Paris P, Irwin G. The stress analysis of cracks handbook. Hellertown, Pennsylvania: DEL Research Corporation; 1973.